

Revealing metals microstructure with TruePix EBSD Technology

How direct electron detection enhances
ease of use and boosts productivity

Electron backscatter diffraction (EBSD) is widely used to detect sub-micron features and deformation mechanisms and to analyze crystal orientations and microstructures. It is a foundational part of SEM-based analytical workflows in both research and industry, commonly used to investigate metal, ceramic, and geologic samples.

Continuous advancements in scanning electron microscope (SEM) detectors, digital imaging, computing power, and user-friendly software have transformed EBSD from a niche, expert-only method into a practical and accessible tool for a broad range of materials research. Similarly, recent advances in detector technologies, such as direct electron detection, have further enhanced ease of use, accessibility, and efficiency in EBSD workflows.

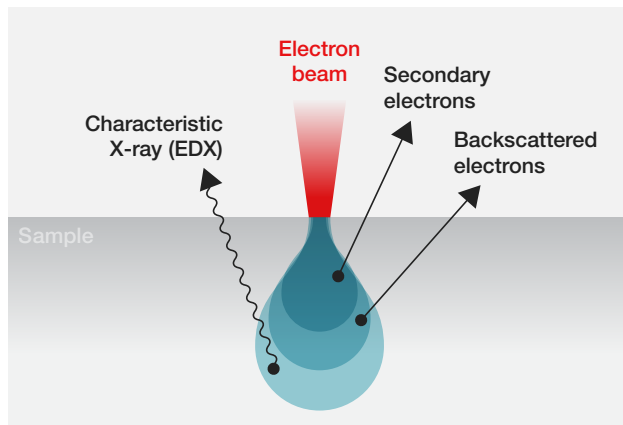
Today, EBSD plays a key role in failure analysis, quality control, and optimizing manufacturing processes, making it indispensable for developing next-generation high-performance materials. As the technique continues to evolve, increasing levels of automation and more intuitive software interfaces will help make EBSD even more approachable for a wider range of users.

Introduction to EBSD

EBSD is a powerful technique used in SEM to analyze the crystallographic structure of a material's surface. But where does the EBSD signal originate, and how is it collected?

To answer this, let's consider a conceptual diagram that illustrates the electron interaction volume, which is the region within a material where incoming electrons from the SEM beam interact with atoms of the sample.

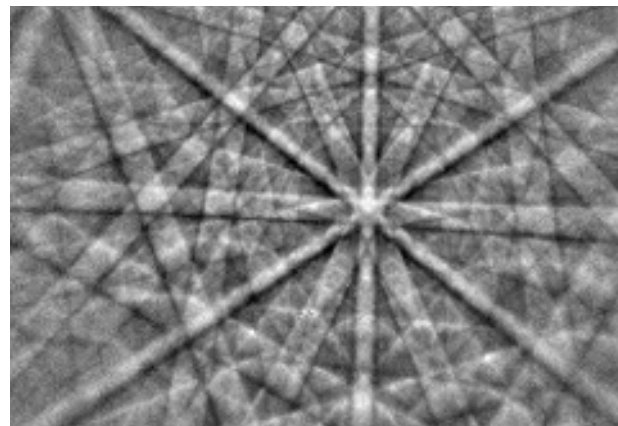
When the electron beam strikes the surface of a sample, it generates a range of signals: secondary electrons, backscattered electrons, characteristic X-rays, and more. Each provides a different type of information about the sample.



Interaction volume between the primary beam and the sample.

EBSD relies specifically on backscattered electrons (BSEs). These are primary electrons from the beam that are scattered back out of the material after elastically interacting with its atomic lattice. Although most BSEs scatter incoherently and are used primarily to highlight differences in atomic weight, a small fraction are diffracted by the crystal planes. These are the electrons that produce EBSD patterns.

Importantly, the useful EBSD signal originates not from the entire interaction volume but from a very shallow region close to the surface, where diffracted BSEs can escape the sample and reach the detector. These diffracted electrons form Kikuchi patterns characterized by sets of bright and dark bands indicative of the underlying crystallographic orientation.



Example of a Kikuchi pattern.

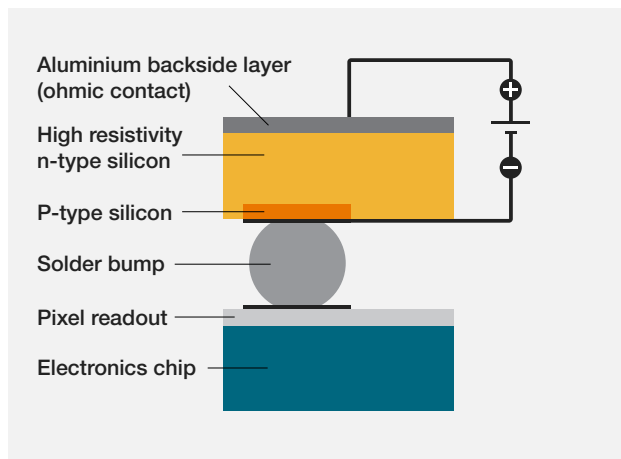
A dedicated EBSD detector captures these patterns. Specialized software then compares them against databases of known crystal structures to determine the orientation and other crystallographic phases of each point analyzed on the sample.

Direct electron detection and TruePix Technology

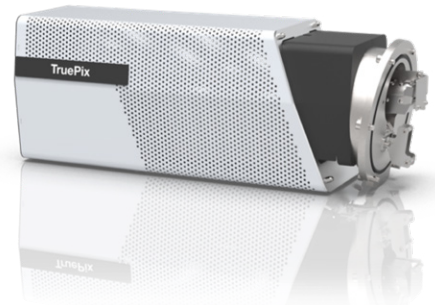
Traditionally, EBSD patterns were captured by an optical camera that recorded diffraction patterns generated by BSEs on a phosphor screen. In this configuration, BSEs struck a scintillating screen, which emitted visible light that was then captured by a CCD or CMOS camera. Although effective, this indirect detection method led to signal loss, optical blurring, and limited acquisition speed.

The advent of direct electron detection (DeD) technology marked a significant advancement. In DeD systems, electrons are captured directly by a sensitive pixelated detector without a phosphor screen or light conversion. This direct approach provides three benefits:

- It improves the signal-to-noise ratio
- It improves data acquisition at lower keVs, ultimately improving the spatial resolution and pattern sharpness
- It enables much faster data acquisition and low-dose measurements for beam-sensitive applications



The hybrid Timepix semiconductor device.



TruePix EBSD Detector.

Thermo Scientific™ TruePix Technology is based on the Timepix detector, a hybrid pixelated detector originally developed at CERN. Unlike traditional optical systems, Timepix detects electrons directly using a pixelated sensor, with each pixel capable of individual signal processing. Timepix technology has enabled significant performance improvements, particularly in challenging EBSD applications like beam-sensitive materials or in-situ experiments.

Main benefits of TruePix Technology

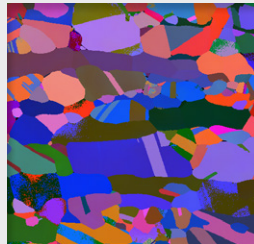
- **High sensitivity and throughput:** Delivers single-electron sensitivity and over 3,000 patterns per second per nanoampere (pps/nA), enabling rapid, high-quality data acquisition even at low beam currents
- **Outstanding low-kV performance and improved spatial resolution:** Optimized for low accelerating voltages and low beam currents, reducing the interaction volume and the beam spread to enable high-resolution analysis of fine-scale structures and beam-sensitive materials
- **Single electron counting for precise dose control:** Accurately counts individual electrons, allowing for fine control over the electron dose, which is critical in low-dose or high-precision applications
- **On-chip electron energy filtering:** Integrated energy filtering at the detector chip level suppresses low-energy electrons, improving Kikuchi pattern contrast and indexing accuracy without the need for additional hardware or post-processing
- **Seamless integration with the SEM platform:** Co-developed with the SEM system to ensure native integration of EBSD and SEM functions, including synchronized beam control, built-in collision avoidance, and a unified user interface for streamlined setup and reliable results

Crystallographic information from EBSD

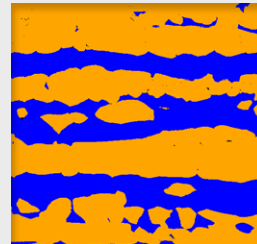
EBSD analysis produces a variety of maps, each highlighting different aspects of a material's microstructure. Together, they provide a comprehensive view of crystallographic structure, deformation, and phase distribution. Below are the most commonly used EBSD maps.



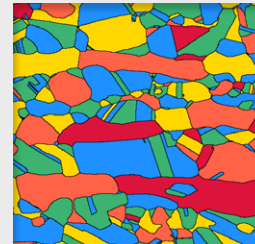
Inverse pole figure (IPF) maps show the crystallographic orientation of grains relative to a reference direction (e.g., normal or rolling direction). These maps are especially useful for visualizing the preferential orientation of grains.



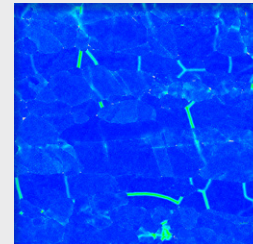
Euler angle maps represent grain orientations using Euler angles (ϕ_1 , ϕ , ϕ_2). Though more abstract than IPF maps, they are important for orientation-based numerical modeling and quantitative analyses.



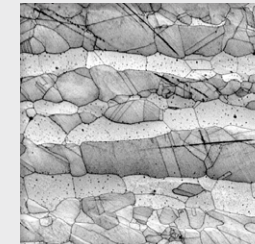
Phase maps identify and color-code different crystal structures or phases present in the sample (e.g., α , β , or intermetallic phases). Phase maps are essential for analyzing multiphase alloys, coated systems, or phase transformations.



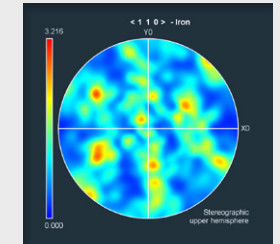
Grain boundary maps highlight the boundaries between grains, including low-angle, high-angle, and twin boundaries. They help assess boundary character and its influence on properties such as corrosion resistance and mechanical behavior.



Kernel average misorientation (KAM) maps show local misorientation within grains and are often used as an indicator of local deformation or dislocation density. They're useful for studying deformed or work-hardened materials.



Pattern quality maps indicate the quality of the EBSD patterns across the scan. Areas with low pattern quality often correspond to rough surfaces, highly deformed zones, or poorly prepared regions.



Pole figures provide a quantitative view of crystallographic texture over the scanned area. These tools are crucial for analyzing anisotropy in mechanical or physical properties and understanding the effects of processes such as rolling, forging, and recrystallization.

Together, these outputs make it possible to establish clear relationships between processing, microstructure, and properties. This capability makes EBSD a key technique in several fields, including alloy development, failure analysis, and advanced materials engineering.

How EBSD connects properties, microstructure, and performance

EBSD is especially valuable in metals research because it offers direct, spatially resolved insight into microstructural features that critically influence material behavior. Processing methods such as rolling, annealing, welding, and additive manufacturing all alter the internal structure of metals, and EBSD helps to visualize and quantify these changes at the grain scale.

EBSD can precisely map and measure key characteristics such as grain size, crystallographic texture, and grain boundary distribution. These microstructural parameters are essential for understanding mechanical properties like strength, ductility, toughness, and fatigue resistance. With EBSD, researchers can establish clear links between processing conditions and microstructure evolution to ultimately improve and enhance the performance of final products.

Sample preparation tips for reliable EBSD in metals

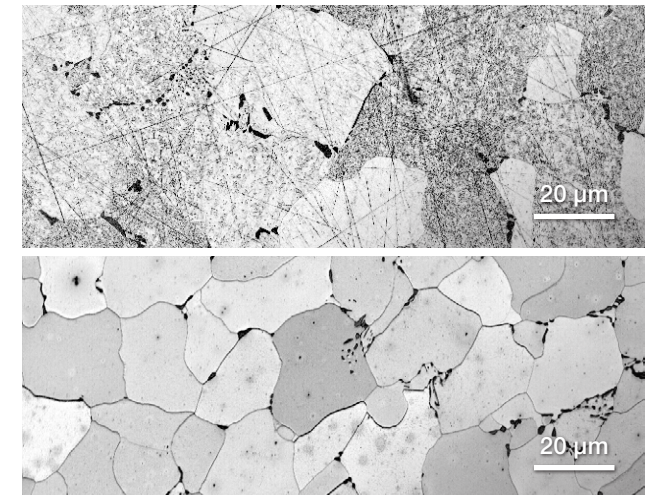
Surface condition plays a defining role in pattern quality and data reliability. To fully leverage EBSD's capabilities, sample preparation must be carried out with great care.

Before selecting a polishing method, consider a few key tips that apply to most metals to help you achieve clean, deformation-free surfaces.

- Tailor pressure and cleaning to the metal: Soft metals like aluminum smear easily, so low pressure and frequent cleaning are required. Hard alloys like tool steels require finer abrasives and longer polishing to fully remove deformation.
- Inspect surfaces frequently: Tiny scratches or smears can degrade pattern quality.
- Minimize contamination: Dust, debris, or polishing residues can reduce indexing accuracy.

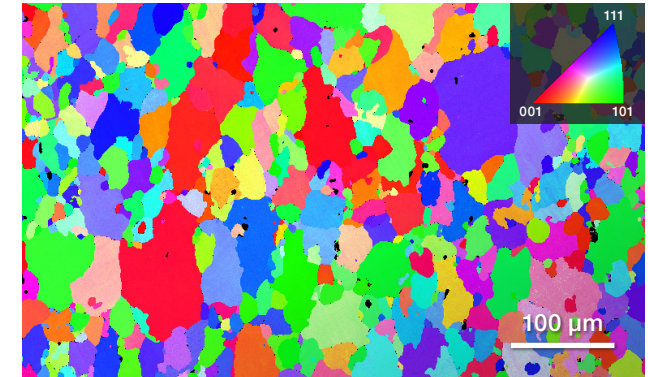
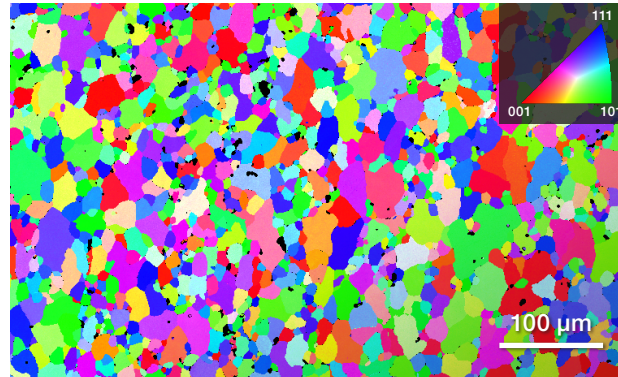
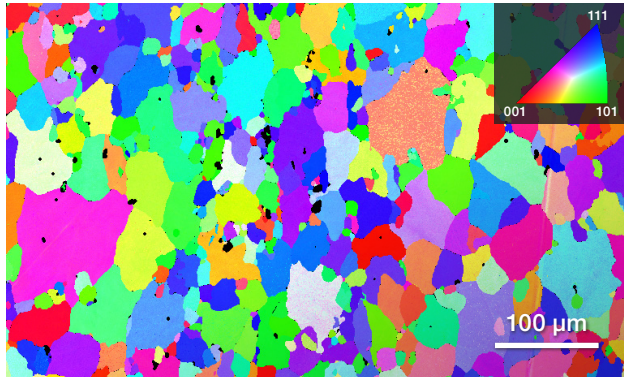
Furthermore, the choice of polishing steps determines the final surface quality.

- Colloidal silica (~0.04 μm) provides a final polish to remove fine scratches and minimize residual mechanical damage.
- Electropolishing is an excellent option for conductive alloys such as steels, Ni-based alloys, and titanium. It removes the deformed layer left by mechanical polishing and produces a stress-free surface.
- Ion polishing (i.e., broad-beam or FIB) is useful for hard or layered materials, or for site-specific work. It must be carefully controlled to avoid artifacts such as curtaining or re-deposition.



Pattern quality maps of AISI 1008 low-carbon steel. The upper map shows results from a silica-polished surface, while the bottom one shows the same material after electropolishing. The comparison highlights how electropolishing improves EBSD results by removing scratches more effectively and minimizing surface deformation and strain.

Case studies in metals characterization using EBSD



Inverse pole figure orientation maps (IPF-X) reveal the different crystallographic orientations of the grains, from left to right, of the T3, T6, and T81 samples.

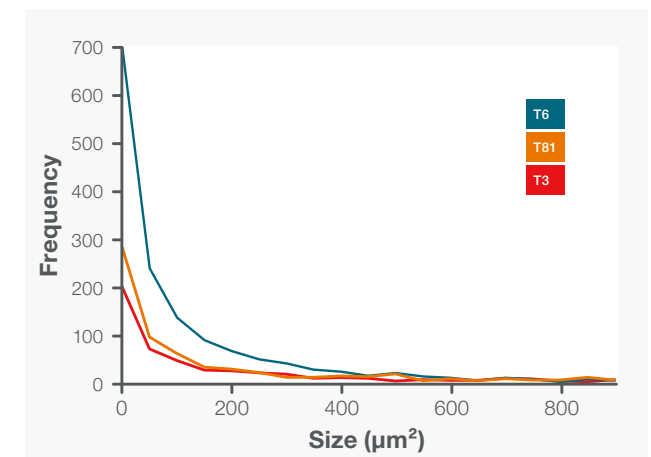
Effect of aging heat treatments on the microstructure and mechanical properties of AA2024 aluminum alloy

Aluminum alloys are widely used in aerospace because of their light weight and corrosion-resistance, with AA2024 being a common choice due to its favorable mechanical properties. This alloy is specifically strengthened by the addition of copper and magnesium, enabling both solid solution strengthening and precipitation hardening.

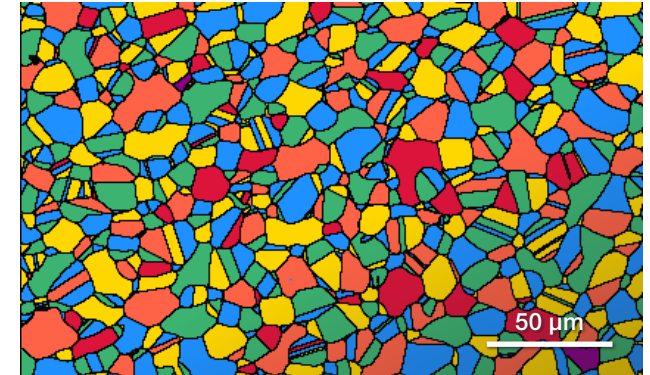
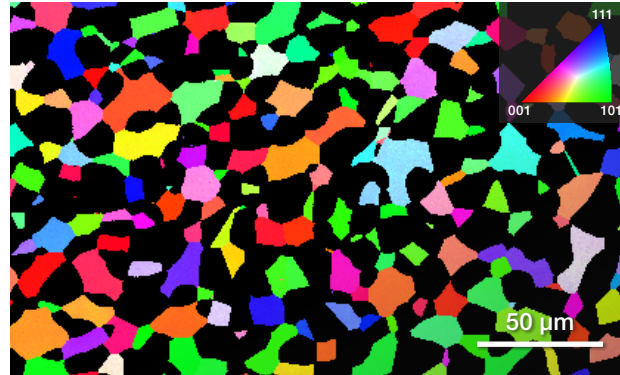
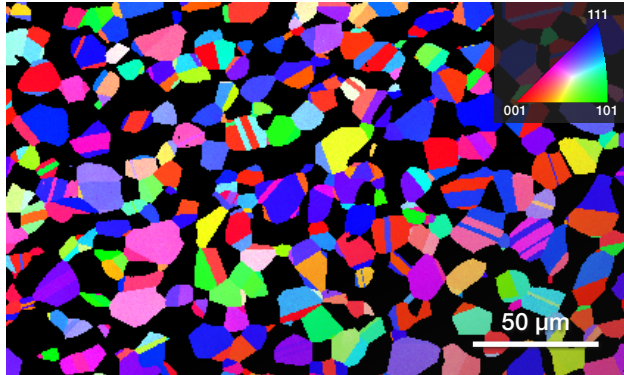
Various treatments are used to tune the mechanical behavior of AA2024 to different applications. For example, three different aging heat treatments, T3, T6, and T81, produce a specific balance of strength and ductility:

- **T3** (heat treated, cold rolled, then naturally aged to a substantially stable condition) preserves the most ductility
- **T6** (heat treated then artificially aged) delivers the highest strength and hardness
- **T81** (heat treated, cold rolled, then artificially aged) provides a balance of strength and ductility

EBSD characterization reveals the grain size distribution and crystal orientation for each treatment, providing insights into how microstructural changes directly relate to mechanical performance. The samples with T3 and T81 treatments display large and relatively uniform grains, with average sizes of $480 \pm 50 \mu\text{m}^2$ and $420 \pm 70 \mu\text{m}^2$, respectively. T6, which was not cold rolled, showed a much smaller grain size of $170 \pm 90 \mu\text{m}^2$.



Grain size distribution for the three different aging treatments.

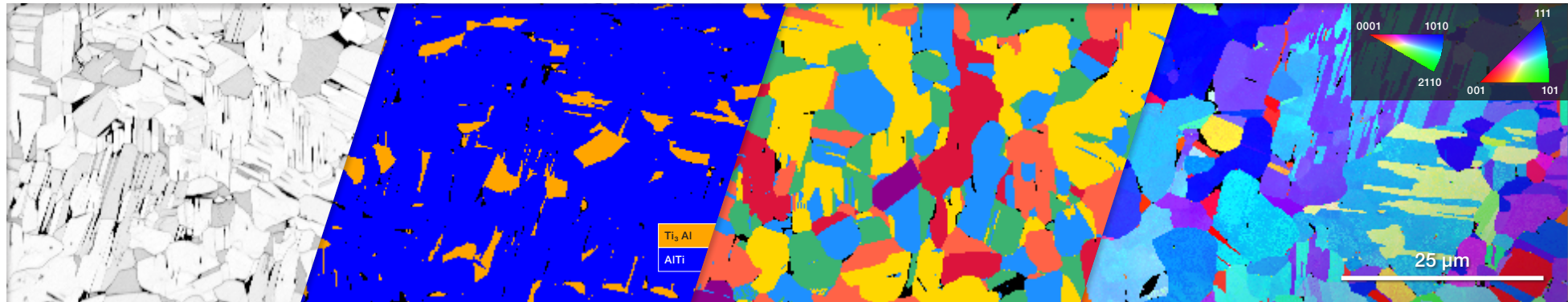


From left to right: IPF-Z maps of the austenite and ferrite phases showing the different orientations and the presence of twinning. The grain map makes it possible to extract information about the size of grains. These analyses were acquired at 6 keV, which made it possible to resolve much smaller features than with higher acceleration voltages, usually employed with the traditional EBSD detectors.

Microstructural characterization of duplex stainless steels for marine applications

Duplex stainless steels are designed to address the limitations of single-phase steels in harsh environments such as marine applications. They contain ferrite and austenite phases in nearly equal proportions, combining the high strength of ferrite (which has a body-centered cubic crystal structure) with the improved ductility of austenite (which exhibits face-centered cubic symmetry). This dual-phase structure also offers excellent resistance to stress corrosion cracking, making these materials highly suitable for fatigue-prone, corrosive environments.

However, optimizing duplex steels for critical applications requires accurate phase quantification and orientation analysis. Thanks to its sensitivity, EBSD with direct electron detection allows for low acceleration voltage characterization, delivering a much higher spatial resolution and providing high-resolution information on phase fractions and crystallographic orientations of ferrite and austenite, visualized in individual IPF-X maps.



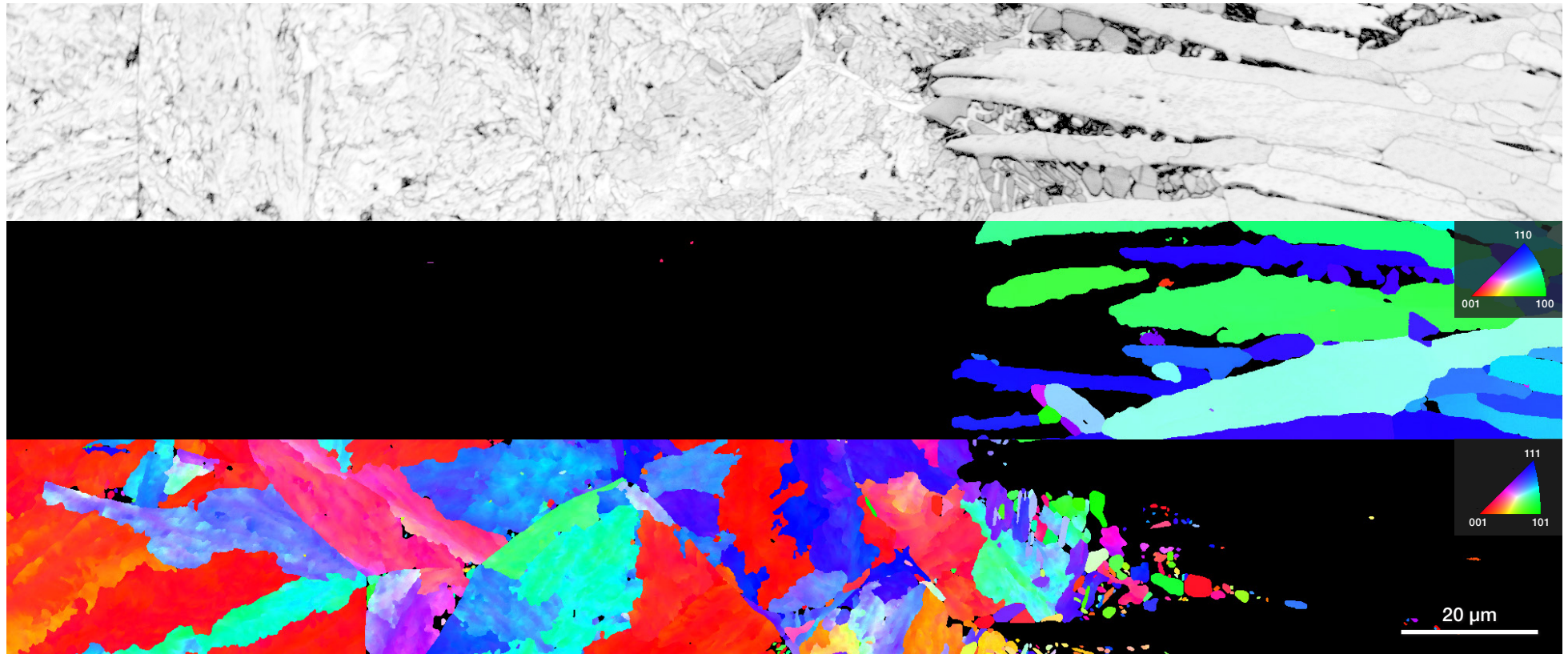
From left to right: Pattern quality, phase, grain, and IPF-X maps.

Grain structure and phase morphology in dual-phase Ti-Al alloys

Titanium alloys play a critical role in aerospace engineering, particularly in high-performance components such as compressor blades, discs, and heat exchangers. These applications demand materials that combine high strength and corrosion resistance while maintaining performance at elevated temperatures.

For example, an additively manufactured titanium aluminide alloy featured a biphasic structure, with γ -TiAl enhancing high-temperature strength and creep resistance and α_2 -Ti₃Al contributing to improved ductility.

To optimize the mechanical performance of this alloy in service conditions, it was essential to understand its phase distribution and morphological characteristics. EBSD characterization revealed that γ -TiAl constitutes 89.4% of the area fraction, forming equiaxed grains, while α_2 -Ti₃Al accounts for 9.4%, appearing in platelet or lath-shaped morphologies.



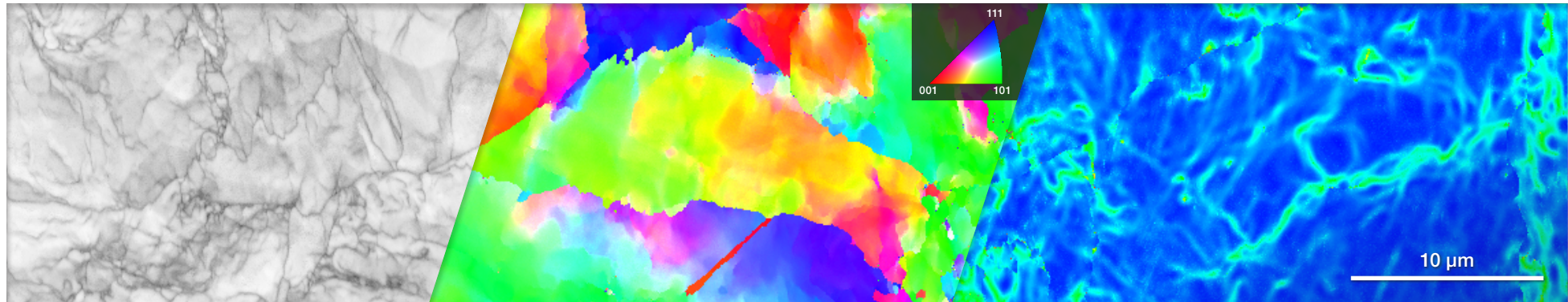
From top to bottom: Pattern quality, IPF-Y map of the Fe₂B phase, and IPF-Y map of the steel.

Analyzing phase formation and grain orientation in boride-coated hardened steel

Hardened steels are essential in wear-resistant industrial components such as cutting tools, gears, pumps, and valves, where durability and reduced friction are critical. Surface coatings like diamond-like carbon (DLC), titanium nitride, and boride are commonly applied to further extend component lifespan.

For example, boride coatings on 4140 steel can form two primary phases: FeB (orthorhombic), which is brittle, and Fe₂B (tetragonal), which is more ductile and mechanically desirable. Understanding the formation, morphology, and distribution of these phases is crucial for optimizing coating performance and ensuring structural reliability. To achieve this, EBSD was used to examine the microstructure within the reaction layer.

The results showed that the desired Fe₂B phase grew inwardly from the reaction surface in a dendritic morphology. Furthermore, inverse pole figure (IPF) maps revealed the preferential crystallographic orientation of grains and indicated uniformity in the large Fe₂B grains in the boride layer, supporting the integrity and effectiveness of the coating.



From left to right: Pattern quality map, IPF-X map, and KAM map.

Evaluating severe plastic deformation in copper using EBSD

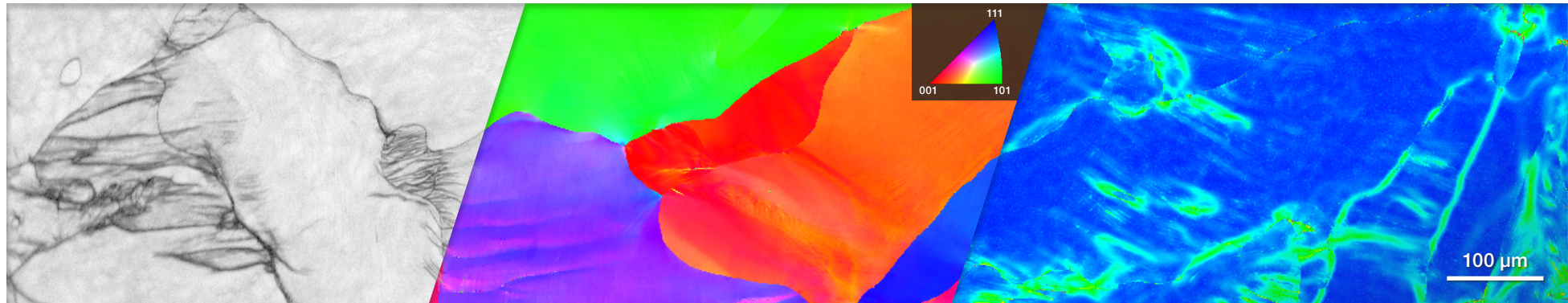
Copper's combination of ductility, corrosion resistance, and high electrical and thermal conductivity makes it indispensable in many functional applications. When subjected to severe plastic deformation, via high-pressure torsion (HPT), for example, its grain structure is significantly altered, leading to large grains with dislocation walls inside.

Traditional characterization methods such as optical microscopy or standard electron imaging cannot resolve the subtle microstructural changes that occur during severe plastic deformation. In contrast, EBSD enables a deeper understanding of the underlying microstructural evolution.

In this case, EBSD reveals key crystallographic features of the deformed copper:

- The pattern quality (PQ) map highlights areas of crystal distortion and dislocation buildup
- The inverse pole figure (IPF-X) map displays the crystallographic orientation of individual grains and shows changes across the microstructure
- The kernel average misorientation (KAM) map provides a quantitative measure of the local angular misorientation, offering insight into the degree of plastic strain experienced by the material

EBSD proved to be a powerful toolkit for quantifying grain refinement and mapping deformation gradients in copper.



From left to right: Pattern quality map, IPF-X map, and KAM map.

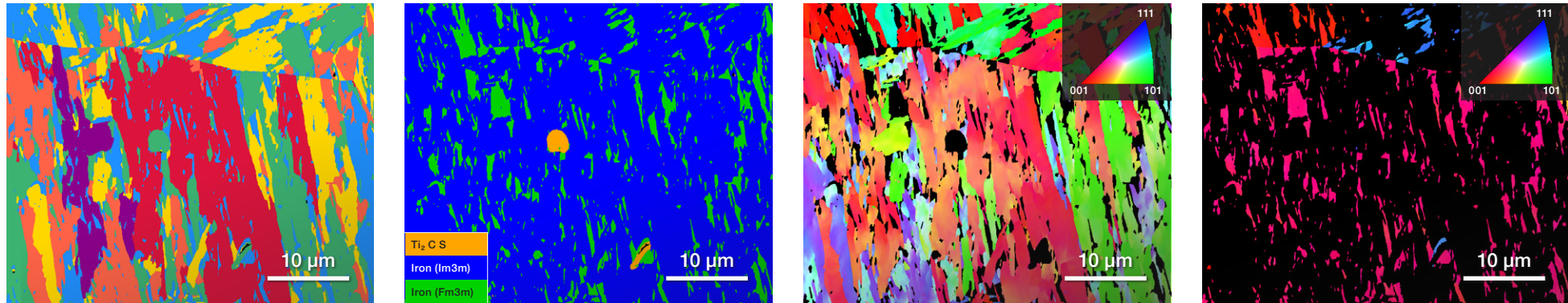
Investigating deformation behavior in a cold-rolled, high-entropy alloy

In high-performance environments where creep resistance at elevated temperatures is essential, high-entropy alloys (HEAs) offer a promising alternative to conventional alloy systems. Their unique composition, built from multiple principal elements, leads to a complex atomic structure and often unpredictable mechanical behavior.

In this case, a cold-rolled HfNbTaTiZr alloy with a body-centered cubic (BCC) crystal structure was characterized to better understand how deformation affects the internal grain structure. The irregular atomic distribution in HEAs makes conventional imaging methods insufficient for resolving fine-scale misorientation and strain.

The pattern quality map shows which patterns have good quality. Low-quality patterns indicate the presence of dislocation. The inverse pole figure (IPF)-X orientation map shows not only the preferred grain orientations but also internal misorientations induced by deformation. The kernel average misorientation (KAM) map quantifies these angular misorientations, providing a direct measure of local strain gradients introduced by cold rolling.

Rather than focusing solely on grain size or boundaries, this analysis highlights internal misorientations that reveal how this complex material accommodates strain. These insights are essential for advancing the mechanical understanding of HEAs.



From left to right: Grain map, phase map, and IPF-Z map of the ferrite and IPF-Z map of the austenite.

Characterizing martensite and austenite in stainless-steel landing gear

Aerospace landing gear components are often manufactured from passivated stainless-steel alloys to eliminate the use of hazardous coatings such as cadmium or chromium, which pose environmental and health risks. These components are typically produced through forging processes that impart high strength and toughness achieved via the controlled formation of martensitic packets within the microstructure. The microstructure preserves a small but critical fraction of retained austenite, which improves the alloy's overall toughness and fatigue resistance.

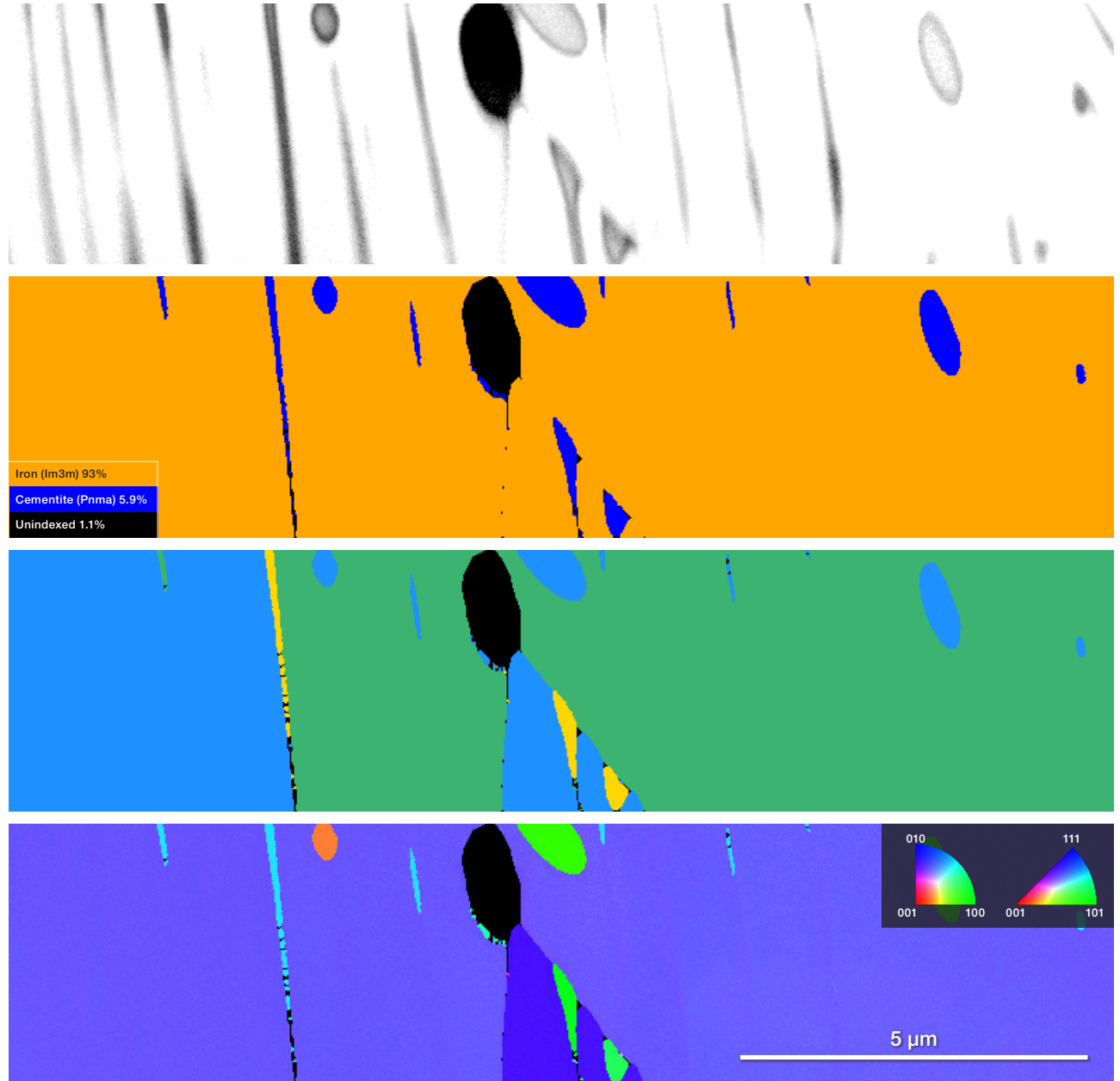
EBSD characterization offers crucial information on this intricate multiphase microstructure. Grain boundary maps reveal the detailed morphology of martensite packets, capturing their complex and often interwoven features. The phase map differentiates the constituent phases, identifying ferrite with its body-centered cubic (BCC) crystal structure, austenite exhibiting face-centered cubic (FCC) symmetry, and various secondary precipitate phases that may influence mechanical behavior and corrosion resistance. And the inverse pole figure (IPF-Z) map of the FCC phase provides detailed crystallographic orientation information on the retained austenite grains.

Together, these EBSD analyses form a comprehensive microstructural characterization that supports the optimization of processing parameters and alloy design for enhanced performance of landing gear components in demanding aerospace applications.

Optimizing high-carbon steels through pearlite microstructure characterization

Pearlite, a fundamental microstructure in high-carbon steels, has a key role in affecting mechanical properties in structural engineering applications. It comprises alternating lamellae of ductile ferrite (α -Fe) and hard cementite (Fe_3C), whose morphology and spacing critically influence strength, ductility, and toughness. By carefully controlling cooling rates during processing, the interlamellar spacing can be manipulated to achieve the desired balance of mechanical performance. Coarser cementite lamellae, for example, are known to enhance toughness, making pearlitic steels ideal for load-bearing components in buildings, bridges, and heavy infrastructure.

Low-kV EBSD characterization (8 kV landing energy) enables high-resolution microstructural mapping. The pattern quality shown here reveals a clear contrast between the ferrite regions, which appear bright due to their simple crystal structure, and the more complex, darker cementite lamellae. This differentiation is further confirmed through phase mapping, which quantifies cementite content at approximately 4.6%, aligning with expected microstructural composition.



From top to bottom: Pattern quality map, phase map, grain map, and IPF-Z map.

Advancing materials science

Electron backscatter diffraction has evolved into a cornerstone technique in materials characterization, offering a wide range of information on crystallography, microstructure, and deformation. As demonstrated in the diverse case studies throughout this eBook, EBSD not only reveals the structural intricacies of metals and alloys but also directly links processing conditions to material performance.

Thanks to the continued advancement of direct electron detection technologies, the TruePix EBSD Detector enables faster, more precise, and more accessible analysis. Whether optimizing aerospace alloys, improving surface coatings, or understanding complex phase interactions, EBSD proves to be an indispensable tool for materials science. As the technique continues to develop, it will remain critical to the design, validation, and innovation of the next generation of advanced materials.

How can we help?



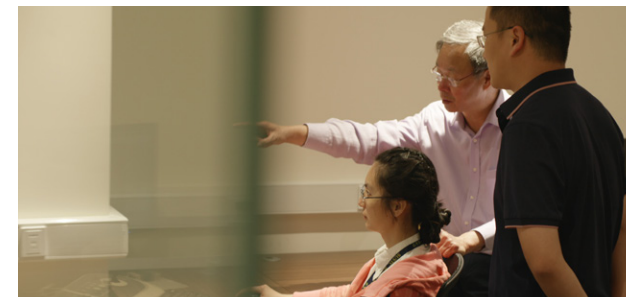
NanoPorts

The teams at our four NanoPorts around the world provide tailored solutions for your applications and on-site or remote demonstrations, plus they act as research collaboration centers. The NanoPorts also help R&D, factory, and field service teams provide optimized outcomes and improved solutions.

[Learn more](#)

Global service logistics and field service assistance

We maintain an extensive network of central warehouses, regional hubs, and local stock locations to fulfill your needs more quickly. From installation services to on-site and remote maintenance agreements, our team of experts is here to support you at every step.

[Learn more](#)

Application support

After your system is installed, our team of applications experts can help you quickly get up to speed. From training and documentation to troubleshooting and more, we're with you every step of the way to help your research succeed.

[Learn more](#)

About Thermo Fisher Scientific

We are the world leader in serving science. Our Mission is to enable our customers to make the world healthier, cleaner and safer.



Learn about the mission of Thermo Fisher Scientific. Duration 1:23.

Our innovative solutions for electron microscopy, surface analysis, and microanalysis help materials science researchers advance their sample characterization to gain deeper insight into the physical and chemical properties of materials from the macroscale to the nanoscale. Our multiscale, multimodal solutions cover a broad range of applications across dozens of industries and research fields, serving customers in academia, government, and industry. Our TEMs, DualBeam™ FIB-SEMs, comprehensive portfolio of SEMs, XPS, and microanalysis solutions, combined with software suites, take customers from questions to usable data by combining high-resolution imaging with physical, chemical, elemental, mechanical, and electrical analysis across scales and modes.

Financial and Leasing Services

At Thermo Fisher Scientific, we will not let budgetary constraints stand between you and your next great discovery.

We are your one-stop partner for the best laboratory products and analytical technologies available, plus the unique financing options you need to accelerate success in science or industry.

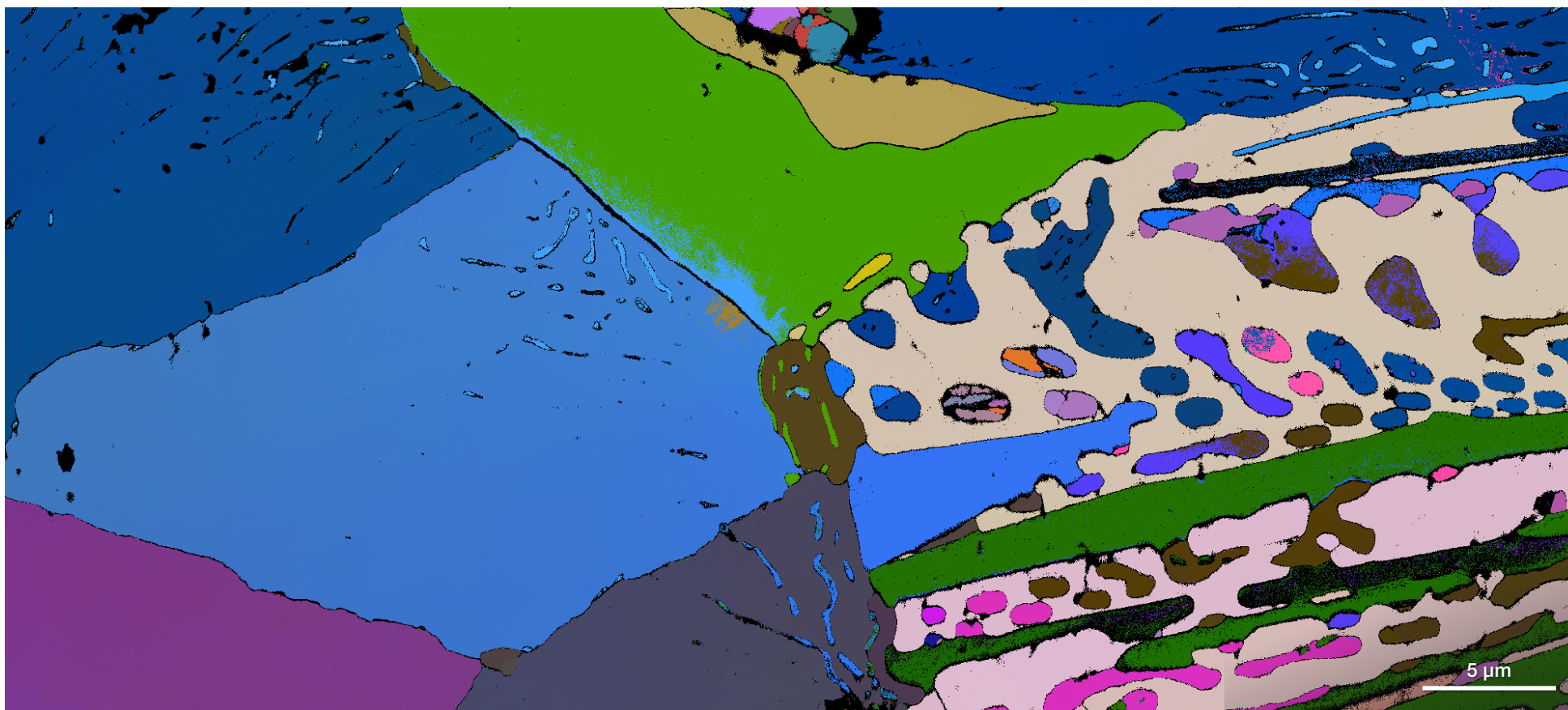
Cost-effective financing designed for each individual customer is key to any successful capital equipment solution.

We understand not just your advanced technology and application requirements, but the business challenges you face when financing your critical equipment assets. For decades, we have worked closely with businesses, hospitals, universities, and municipalities to provide flexible financing terms to support their successful operations.

If you are looking for off-balance sheet financing, accelerated ROI, technology protection, or cash flow management, our innovative financing options can help meet your company's budgetary needs and bottom-line goals.

We also offer instrument maintenance and training services.

**Explore equipment
leasing and
financing options**



Euler map of cast iron.

Learn more at thermofisher.com/truepix

thermoscientific

For research use only. Not for use in diagnostic procedures. For current certifications, visit thermofisher.com/certifications

© 2025 Thermo Fisher Scientific Inc. All rights reserved. All trademarks are the property of Thermo Fisher Scientific and its subsidiaries unless otherwise specified. BR0214-EN-10-2025